Three-dimensional velocity analysis combining ion imaging with Doppler spectroscopy: Application to photodissociation of HBr at 243 nm

Tohru Kinugawa and Tatsuo Arikawa

Citation: The Journal of Chemical Physics **96**, 4801 (1992); doi: 10.1063/1.462766
View online: http://dx.doi.org/10.1063/1.462766
View Table of Contents: http://scitation.aip.org/content/aip/journal/jcp/96/6?ver=pdfcov
Published by the AIP Publishing

LETTERS TO THE EDITOR

The Letters to the Editor section is divided into four categories entitled Communications, Notes, Comments, and Errata. Communications are limited to three and one half journal pages, and Notes, Comments, and Errata are limited to one and three-fourths journal pages as described in the Announcement in the 1 January 1992 issue.

COMMUNICATIONS

Three-dimensional velocity analysis combining ion imaging with Doppler spectroscopy: Application to photodissociation of HBr at 243 nm

Tohru Kinugawa and Tatsuo Arikawa
Department of Applied Physics, Faculty of Technology, Tokyo University of Agriculture and Technology, Koganei-shi, Tokyo 184, Japan

(Received 9 September 1991; accepted 31 December 1991)

Investigations of molecular dynamics often require the measurement of the full three-dimensional velocity distribution of low energy products.[1,2] For the angle-resolved experiment, there have been two efficient and sensitive velocity analyzing methods using the laser-probing technique: the Doppler and the ion imaging techniques.

The Doppler technique is based on line-shape analysis to get one-dimensional information of the velocity distribution.[3] A Doppler-broadened spectrum probed by a laser provides the projection of the three-dimensional velocity distribution onto the axis of the laser beam. A complicated calculation procedure is needed to reconstruct the three-dimensional velocity distribution. It is only for a few simple velocity distributions that this technique provides reliable information, e.g., completely isotropic velocity distributions or axially symmetric velocity distributions. In the case of the photofragmentation, the angular distribution $f(\theta)$ of the fragments is an axially symmetric distribution described in the form of a simple sinusoidal function as

$$f(\theta) \propto 1 + \beta \cdot P_2(\cos\theta), \tag{1}$$

where θ is the angle between the recoil direction of the fragments and the polarization of the photolysis light, β is the anisotropy parameter and P_2 is the second Legendre polynomial. Therefore, the Doppler technique has been successful in determining the velocity of the photofragments, especially of the fast H fragments.[4] However, for the full three-dimensional analysis by the Doppler technique, an elaborate experimental setup is needed.[5]

The "ion imaging" is a newly developed velocity analyzing technique to visualize the velocity distribution.[6,7] This technique provides two-dimensional projections of the three-dimensional velocity distribution onto an imaging surface. The projected distribution is converted into a fast optical image, which is taken by an image detector, such as a CCD camera or an image intensifier. This method is able to measure the mass, the speed and the angular distributions of photofragments simultaneously even with a single laser pulse. The ion imaging has been applied to the photolysis experiments[8] as well as the bimolecular reaction experiments.[9]

Although the ion imaging has made progress over the limitations of the Doppler technique, a purely three-dimensional velocity analyzing method is still needed for two main reasons. First, the numerical procedures to reconstruct the three-dimensional distribution do not always provide reliable information. Numerical procedures based on linear mathematics are likely to bring about "ghost" signals if there are any errors or fluctuations in the experimental data. The typical causes of these troubles are the finite dynamic range of the detector, the nonuniformity of a position-sensitive detector, or the errors in the geometrical setup of the experiment. These troubles can be checked and avoided immediately without numerical procedures if the three-dimensional distribution is directly visualized in the image. Second, the ion imaging may be more effective for surface experiments. Interesting angular distributions far from axial symmetry were reported in electron-stimulated-desorption (ESD) experiments[10] or surface-molecular beam scattering experiments.[11] The ion imaging technique cannot be applied to these surface experiments straightforward because its numerical procedure is only applicable to axial symmetric distributions.

In this paper we report a simple and reliable way of combining the one-dimensional Doppler technique with a two-dimensional imaging technique to obtain a cutout view of the three-dimensional velocity distribution (hereafter, we refer to this technique as the "Doppler-imaging" technique). This technique was tested experimentally by the photolysis study of an HBr molecular beam at 243 nm. The image of the H photofragments clearly shows that there are two distinct dissociation pathways for this molecule: $H + Br(^2P_{3/2})$ and $H + Br(^2P_{1/2})$. These pathways could not be distinguished from each other by conventional Doppler spectroscopy.[12]

A schematic view of the principle is presented in Fig. 1. The narrow band probe laser ionizes H atoms of a given velocity component Vz along the axis of the probe laser propagation. The images of fast H fragments taken by the geometry of the previous ion imaging are presented in Fig. 4 of Ref. 13. Our experimental geometry is different from that of Ref. 13 in respect to the direction of the laser; the laser beam goes almost parallel to the axis of the time-of-flight tube. The velocity component Vz is determined from

 0021-9606/92/064801-04$06.00

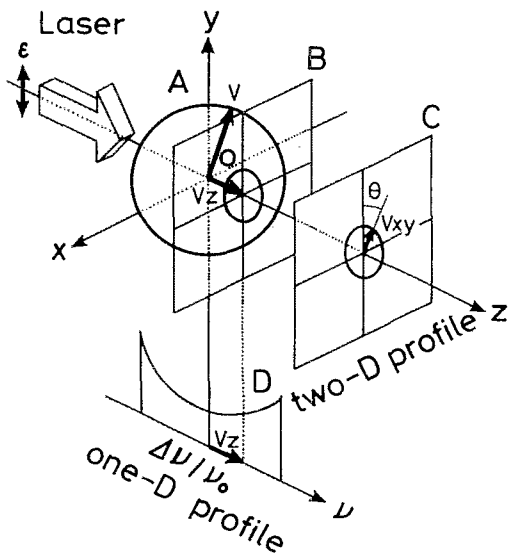

FIG. 1. Schematic view to show the principle of "Doppler-imaging" technique. Laser beam propagating along z axis produces H ions at the scattering point (O). Vz is determined from the Doppler shift in the spectrum (D). Vxy is determined from the image of H ions (C). θ is the angle between the recoil velocity of fragment H atoms and the polarization vector of the laser.

the Doppler shift as

$$Vz = c \cdot (\nu - \nu_0)/\nu_0, \tag{2}$$

where c is the speed of light, ν is the frequency of the probe laser and ν_0 is the resonance frequency of atoms at rest. The velocity component Vxy transverse to the probe laser direction can be determined from the arrival position of ions on the image surface by the following relation:

$$Vxy = R/T, \tag{3}$$

where R is the distance from the image center and T is the flight time of the ions. Images are taken by a gated image intensifier (GII). T is experimentally defined by the timing of the gate pulse to the GII. Since the ion of interest undergoes free drift in both X and Y directions, the angular distribution in the XY plane is directly visualized in the image. Thus the image with a given probing frequency provides a cutout view of the three-dimensional velocity distribution. No elaborate calculation is necessary to derive the three-dimensional information from these obtained images. When the frequency of the probe laser is scanned over the Doppler broadened spectrum, different cutout views of the three-dimensional velocity distribution are obtained, and the full three-dimensional map is reconstructed from these views.

A photolysis experiment on an HBr molecular beams was performed to test the new technique. This sample has some features appropriate for the test. First, the Doppler shift of the fragment H atom is sufficiently large (150 GHz for a translational energy of 1.3 eV) to use the Doppler technique. Second, in the case of diatomic molecules, the angular and the speed distributions of photofragments are very simple, purely parallel or purely perpendicular to the polarization vector of the laser, provided dissociation proceeds much faster than the rotation of parent molecules[14] and there are no curve crossings. A comparison of theoretical and experimental data is possible to check the performance of the analyzer. Concerning the molecular process of HBr, another interesting aspect should be mentioned: two dissociation pathways were hitherto reported[15] and different anisotropy parameters were theoretically anticipated for these pathways.[16]

Our experimental setup is very similar to that in the previous paper[7] and will be described briefly here. The apparatus consists of a molecular beam source, a time-of-flight mass spectrometer and an image acquisition system. An effusive beam of HBr molecules passes the ionization region, where a static electric field is applied to accelerate product ions. Ultraviolet light at 243 nm from a pulsed laser intersects the beam at right angles. This laser beam dissociates HBr molecules and ionizes the fragment H atom resonantly within the 10 ns pulse duration. The accelerated ions are detected by a microchannel plate with a phosphor screen. The image of each light spot is intensified by GII and its output image is taken by a CCD camera. The video signal from the CCD camera is processed by a home-made digital circuit to detect the positions of the light spots. The position data are put into the memory of a personal computer. This detection system has the sensitivity to detect even single ions. There are a few significant changes added to the previous experimental setup. The directions of molecular and laser beams relative to the TOF axis were changed; the laser beam now goes parallel to the TOF axis and the molecular beam goes perpendicular to the TOF axis. The molecular beam of HBr is prepared from an effusive nozzle of a stainless tube (0.3 mm-diam) which is set parallel to the electrodes to minimize the disturbance to the uniform acceleration field. The laser beam is introduced into the ionization region from the back of the ion-repeller to propagate almost parallel to the TOF axis. The laser propagation is inclined slightly downward ($\sim 6°$) to the TOF axis to avoid irradiation of the MCP surface. The image distortion due to this inclination is less than 0.5% and is ignored in the analysis. The laser beam is focused about 2 mm downstream from the nozzle tip and no further effort is attempted to collimate the molecular beam because the initial velocity of the thermal HBr molecule is much slower than that of the fragment H atom ($\sim 1/40$) and influences very little the spatial resolution of the image. The laser frequency (band width 10 GHz) is tuned to the two-photon transition of the H atom ($1s\,^2S_{1/2} \rightarrow 2s\,^2S_{1/2}$), where the line broadening by the Doppler effect is estimated to be about 150 GHz. Since our experiment is one color, the laser beam serves to dissociate HBr and to ionize the fragment H atoms simultaneously. Although the photoabsorption cross section of the HBr molecule is small ($\sim 10^{-19}$ cm^2)[17] at this wavelength, the laser fluence of 0.3 mJ is enough to observe the following fragment images. The experimental results are shown in Fig. 2. Each image in Fig. 2 is accumulated for 4000 laser shots and obtained at different laser frequencies. Figure 2(a) is the image when H atoms of $Vz = 0$ are selectively

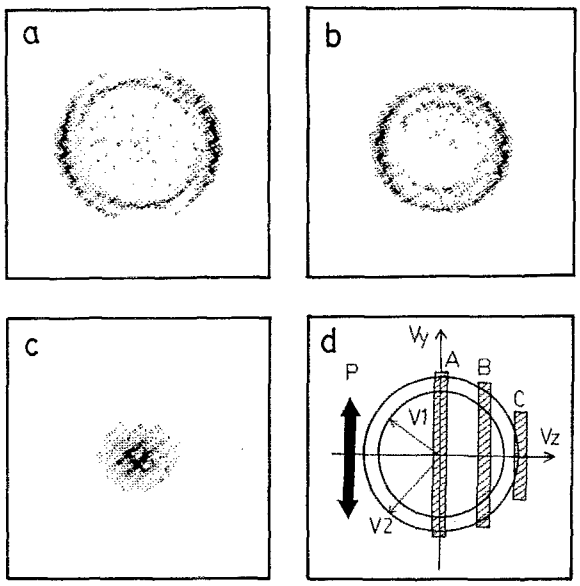

FIG. 2. Images of photofragment H atoms generated from the photodissociation of HBr at 243 nm. (a) $\Delta\nu = 0$ GHz. (b) $\Delta\nu = 35$ GHz. (c) $\Delta\nu = 70$ GHz. (d) Hatched regions represent positions of velocity regions selected by the Doppler technique. P is the polarization vector of the laser. $V1$ and $V2$ are the radii of H^+ images produced from the two dissociation channels in the text.

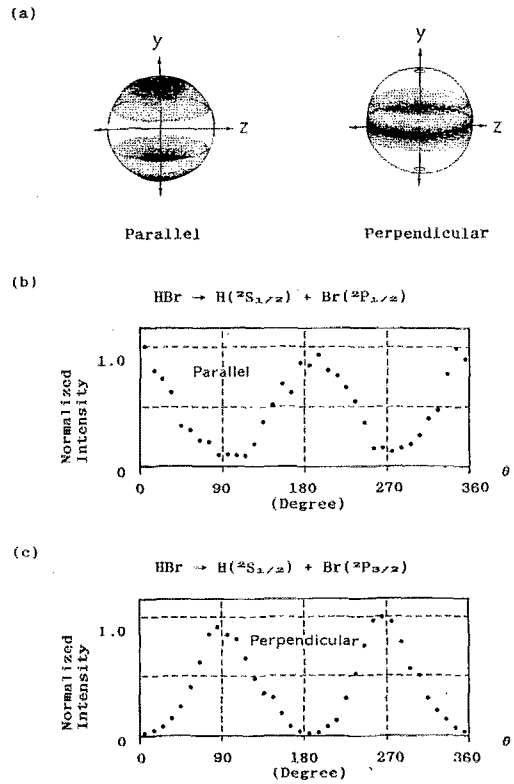

FIG. 3. Schematic representations of three-dimensional distribution of photofragments and experimental angular distributions obtained from Fig. 2(a). (a) Three-dimensional distribution of photofragments: parallel transition (left) and perpendicular transition (right). The polarization vector of the laser is parallel to y axis. The TOF axis and the laser beam are parallel to z axis. (b) The angular distribution to the inner circle of Fig. 2(a). (c) The angular distribution to the outer circle of Fig. 2(a).

ionized. Two rings are clearly seen here. These two rings correspond to the two different pathways dissociating to different atomic states: the ground level of $Br(^2P_{3/2})$ and the spin–orbit excited level of $Br^*(^2P_{1/2})$. The angular distribution patterns of these two components also show a remarkable contrast to each other. Since the polarization vector of the laser lies vertically in Fig. 2(a), the inner ring shows a parallel transition while the outer ring shows a perpendicular transition. These anisotropies are explained by the correlation between the molecular electronic states and the levels of the separated atoms.[18] The inner ring corresponds to the transition to $^3\Pi_{0^+}$ dissociating to $H(^2S_{1/2}) + Br(^2P_{3/2})$, and the outer ring corresponds to $^3\Pi_1$ dissociating to $H(^2S_{1/2}) + Br(^2P_{1/2})$. The images in Figs. 2(b) and 2(c) are also cutout views of the full three-dimensional velocity distribution with different laser frequencies. Figure 2(d) shows the positions of the velocity regions selected by the Doppler technique. The angular distribution of photofragments generated from the photolysis of diatomic molecules is purely parallel ($\beta = 2$) or purely perpendicular ($\beta = -1$) when the dissociation proceeds much faster than the rotation of parent molecules and there are no curve crossings. The dissociation life time of HBr (~ 5 fs) is much shorter than the rotational period (~ 0.5 ps) of the parent HBr molecules. For the inner circle in Fig. 2(a), the angular distribution is considered to be purely parallel and is given as

$$f(\theta) \propto \cos^2 \theta. \tag{4}$$

For the outer circle in Fig. 2(a), the angular distribution is considered to be purely perpendicular and is given as

$$f(\theta) \propto \sin^2 \theta. \tag{5}$$

These two distributions are schematically described by Fig. 3(a); the parallel transition should be seen as two "mushroom caps" along the y axis of Fig. 3(a), and the perpendicular transition should be seen as an "equatorial belt" in Fig. 3(a). When these distributions are cut out with a median plane of $Vz = 0$, the angular distributions in this cutout view are written in the form of Eqs. (4) and (5).

The experimental results corresponding to those just discussed above are obtained from Fig. 2(a) by plotting signal intensities along the inner and the outer circles, respectively. The cutout plane of Fig. 2(a) is $Vz = 0$ in Fig. 1 because the laser frequency is tuned to the center of the Doppler profile. The results are shown in Figs. 3(b) and 3(c). The most dominant factor causing experimental errors is the production of hydrogen atoms from the photolysis of the background hydrocarbons. The contribution from this factor is seen as a broad circular background image in Fig. 2(a). This contribution was quantified and was subtracted in obtaining Figs. 3(b) and 3(c). Agreement between experimental results and Eqs. (4) and (5) is satisfactory.

The speeds of H atoms via the two dissociation pathways are also determined from the diameters of these two circles in Fig. 2(a) by using Eq. (2). The experimental

results are 1600 m/s and 1350 m/s for the outer and inner circles, respectively. Given the photon energy of 5.14 eV, the bond energy of 3.84 eV[15] and the energy difference between Br and Br* of 0.46 eV, the speeds of H atoms are calculated to be 1580 m/s and 1270 m/s for the outer and the inner circles, respectively. These values agree with the experimental results within experimental errors. When the laser frequency is scanned over the Doppler broadened region of the spectrum, the plane to cut out the three-dimensional velocity distribution moves along the z axis of Fig. 1. As the cutout plane gets more away from the center of the distribution, the diameters of the rings gradually decrease and the perpendicular component becomes more dominant than the parallel component in the image. This description agrees qualitatively with Figs. 2(b) and 2(c). In the case of photofragmentation, the single image of Fig. 2(a) is sufficient to reconstruct the three-dimensional distribution because the fragment distribution must be axially symmetric around the polarization vector of the photolysis light.

The branching ratio of the two dissociation channels is also obtained from Fig. 2(a). The detection efficiency η of photofragments depends on the anisotropy parameter β as well as the velocity v of the fragments. This dependence is expressed in an analytical form after a simple geometrical calculation as given by

$$\eta \propto (4+\beta)\sin\Theta_D - \beta\sin^3\Theta_D, \tag{6}$$

where $\sin\Theta_D = c\cdot\Delta\nu/v$, $\Delta\nu$ is the band width of the laser. Taking this efficiency into account, the branching ratio of $(H + Br^*)/(H + Br)$ is determined to be 0.12.

The present "Doppler-imaging" technique is expected to have a wide range of applications. This technique allows reconstruction of three-dimensional velocity distributions of any symmetry, while the Doppler technique or the imaging technique are only applicable to velocity distributions with an axial symmetry. The velocity distribution can be obtained without any complicated procedures in the present technique. Crossed-molecular-beam experiments and surface analysis by molecular beams are among promising applications. To the species slower than the H fragments of the present experiment, it is difficult to apply the optical Doppler technique because they do not show substantial Doppler shifts. This is, however, rather an advantage for the time-of-flight Doppler technique[19,20] because the velocity selection by the time of flight is easier for slower species.

The authors are indebted to Professor M. Kawasaki and Dr. Y. Matsumi of Hokkaido University for their advice on the photolysis of HBr. The technical support by Messers T. Sato, T. Kodaka, and H. Suzuki is also acknowledged. This work was financially supported by a Grant-in-Aid from the Ministry of Education, Science and Culture of Japan.

[1] G. E. Busch, R. T. Mahoney, R. I. Morse, and K. R. Wilson, J. Chem. Phys. **51**, 449 (1969).
[2] *Atomic and Molecular Beam Methods*, edited by G. Scoles (Oxford University, New York, 1988), Vol. 1.
[3] R. N. Zare and D. R. Herschbach, Proc. IEEE **51**, 173 (1963).
[4] R. Schmiedl, H. Dungan, W. Meier, and K. H. Welge, Z. Phys. A **304**, 137 (1982).
[5] N. Shafer and R. Bersohn, J. Chem. Phys. **94**, 4817 (1991).
[6] D. W. Chandler and P. L. Houston, J. Chem. Phys. **87**, 1445 (1987).
[7] T. Kinugawa and T. Arikawa, Rev. Sci. Instrum. (submitted).
[8] D. W. Chandler, M. H. M. Janssen, S. Stolte, R. N. Strickland, J. W. Thoman, Jr., and D. H. Parker, J. Phys. Chem. **94**, 4839 (1990).
[9] M. A. Buntine, D. P. Baldwin, R. N. Zare, and D. W. Chandler, J. Chem. Phys. **94**, 4672 (1991).
[10] H. Daimon and S. Ino, Vacuum **41**, 215 (1990).
[11] R. D. Levine and R. B. Bernstein, *Molecular Reaction Dynamics and Chemical Reactivity* (Oxford University, New York, 1987). For the review of investigations to study molecular beam-surface interaction, see Sec. 6.4 and 7.5 of this book.
[12] Y. Matsumi, K. Tonokura, and M. Kawasaki, J. Chem. Phys. **93**, 7981 (1991).
[13] J. W. Thoman, Jr., D. W. Chandler, D. H. Parker, and M. H. M. Janssen, Laser Chem. **9**, 27 (1988).
[14] C. Jonah, J. Chem. Phys. **55**, 1915 (1971).
[15] Z. Xu, B. Koplitz, and C. Witig, J. Chem. Phys. **87**, 1062 (1987).
[16] R. S. Mulliken, Phys. Rev. **51**, 310 (1937).
[17] J. B. Nee, M. Suto, and L. C. Lee, J. Chem. Phys. **85**, 4919 (1986).
[18] The correlation diagram of HBr is the same as that of HCl, i.e., Fig. 3 of Ref. 8.
[19] T. Kinugawa, T. Sato, T. Arikawa, Y. Matsumi, and M. Kawasaki, J. Chem. Phys. **93**, 3289 (1990).
[20] H. J. Krautwalt, L. Schnieder, and K. H. Welge, and M. N. R. Ashfold, Faraday Discuss. Chem. Soc. **82**, 99 (1986).